NASA TECHNICAL NOTE

NASA TN D-6937

NASA TN D-6937

HODOGRAPHIC APPROACH TO PREDICTING INELASTIC STRAIN AT HIGH TEMPERATURE

by Avraham Berkovits

Lewis Research Center
Cleveland, Ohio 44135

NATIONAL AERONAUTICS AND SPACE ADMINISTRATION • WASHINGTON, D. C. • SEPTEMBER 1972

1. Report No.	2. Government Accession No.	3. Recipient's Catalog No.
NASA TN D-6937		

4. Title and Subtitle	5. Report Date
HODOGRAPHIC APPROACH TO PREDICTING INELASTIC STRAIN AT HIGH TEMPERATURE	September 1972
	6. Performing Organization Code
7. Author(s)	8. Performing Organization Report No.
Avraham Berkovits	E-6933
	10. Work Unit No.
9. Performing Organization Name and Address	501-21
Lewis Research Center National Aeronautics and Space Administration Cleveland, Ohio 44135	11. Contract or Grant No.
	13. Type of Report and Period Covered
12. Sponsoring Agency Name and Address	Technical Note
National Aeronautics and Space Administration Washington, D.C. 20546	14. Sponsoring Agency Code

15. Supplementary Notes

16. Abstract

An experimental study of the effect of continuous and discontinuous changes in strain rate on the relationship among strain rate, strain, and stress is described. Data from Udimet 700 in tension at 925° C were used in order to relate cyclic tensile creep to the monotonic properties of the material by means of the hodograph. The nature of modifications caused to the hodograph by discontinuous variation of the strain rate was determined from tests. Reloading at discontinuous strain rate caused reactivation of primary creep. A simple method, based on monotonic material properties, is proposed for predicting cyclic tensile creep response. Preliminary results of cyclic tests agree with predicted response.

17. Key Words (Suggested by Author(s))
Mechanical behavior of materials
Creep
Fatigue

18. Distribution Statement
Unclassified - unlimited

19. Security Classif. (of this report)	20. Security Classif. (of this page)	21. No. of Pages	22. Price*
Unclassified	Unclassified	34	$3.00

* For sale by the National Technical Information Service, Springfield, Virginia 22151

HODOGRAPHIC APPROACH TO PREDICTING INELASTIC STRAIN AT HIGH TEMPERATURE

by Avraham Berkovits

Lewis Research Center

SUMMARY

The effect of rate-dependent processes on low-cycle fatigue life is a major problem at elevated temperatures. Past research has shown that in the elevated-temperature environment a characteristic relationship among strain rate, strain, and stress exists for many materials, as long as changes in strain rate are gradual. This report describes an experimental study of the effect of large changes in strain rate on the characteristic relationship among strain rate, strain, and stress for Udimet 700 at 925° C. An attempt was made to relate cyclic creep phenomena, in terms of instantaneous strain rate, to the monotonic properties of the material. The monotonic relationship among strain rate, strain, and stress at constant elevated temperature is presented in the form of a hodograph, prepared from data obtained in stress-strain tests conducted under constant strain rate to failure. Material flow behavior under a number of noncyclic loading paths was computed from the hodograph and compared with experimental data for Udimet 700. This was done to verify the characteristic relationship among the parameters under such loading paths for the material.

The investigation was extended to conditions common to cyclic tension situations in which rapid load changes occur. The approach taken was the same as for noncyclic conditions. Stress-strain tests were conducted with discrete variation of the strain rate, to determine the nature of the modifications thereby caused to the hodograph.

A simple method, based on the hodograph, is tentatively proposed for predicting cyclic creep response. According to the method, decrease and continuous increase in strain rate result in monotonic-type response. Discrete increase in strain rate reactivates primary flow behavior. Results of preliminary cyclic tests in tension are in agreement with the response predicted.

INTRODUCTION

A major problem in predicting low-cycle fatigue at elevated temperatures has been estimating the effect on life of deformation processes which are strongly rate dependent. These include creep while strain is either increasing or decreasing in the fatigue cycle and stress relaxation while the strain is held constant (fig. 1). Success in estimating low-cycle fatigue life under such conditions has varied considerably (see bibliography in ref. 1). Methods of analysis developed at NASA include (1) the 10-percent rule (ref. 2) and (2) the separate calculation and subsequent summation of the time-independent (fatigue) damage and the time-dependent (creep) damage (refs. 3 and 4). More recently a strain-partitioning approach has been suggested whereby the cyclic strain increment is divided into its constituent components of time-independent and time-dependent deformation (ref. 1).

Another fundamental variable, whose significance is well recognized although not fully explored, is the strain rate, which is related to the cyclic frequency. Strain rate has been shown (ref. 5) to be the controlling variable in many situations involving monotonic creep and might also be expected to have an important influence in cyclic problems.

The strain-rate approach used in analyses of noncyclic situations presumes that the response of a material which behaves inelastically is defined by inelastic strain rate, inelastic strain, and stress. If the relationship among these three parameters is known for a material at a given temperature, it is theoretically possible to predict its flow behavior under any imposed conditions at that temperature. Therefore, given the instantaneous values of the three parameters for a material, the future deformation of the material, be it stress-strain, creep, stress relaxation, or some combination of these, can be predicted independently of knowledge of the prior history. A broader concept of this approach, including temperature as a fourth variable, was originally proposed by Ludwik (ref. 6) and popularized by Hollomon (ref. 7) as the "mechanical equation of state." The temperature parameter usually appears as an exponential function. Under isothermal conditions the mechanical equation of state is of particular value because it permits use of data obtained under one set of conditions, say stress-strain tests at constant strain rate, to predict the response under other conditions, such as creep or stress relaxation.

Experimental substantiation of the equation of state has been limited and inconclusive (ref. 5), and a number of attempts have been made to discredit the concept on theoretical grounds. However, the concept continues to be useful for those materials which are not susceptible to age-hardening or age-softening effects and in the range of temperatures throughout which the specific material is structurally stable. For such materials the equation-of-state concept affords ease of application and reasonable accuracy in calculating monotonic loading paths. Use of the concept to predict behavior under cyclic conditions is less accurate because cyclic loading often involves substantial discrete changes in the strain rate during load reversal and introduces cyclic hardening and softening

effects. Discrete changes in strain rate will be shown to cause a response which is different from the characteristic monotonic response of the material.

This report describes an experimental study of the effect of changes in strain rate on the characteristic relationship among strain rate, strain, and stress. An attempt was made to relate cyclic creep phenomena to the monotonic properties of the material in terms of instantaneous strain rate. The monotonic relationship among strain rate, strain, and stress at constant elevated temperature is presented in the form of a hodograph (ref. 8), conveniently prepared from data obtained in stress-strain tests conducted under constant strain rate to failure. Material flow behavior under a number of noncyclic loading paths was computed from the hodograph and compared with experimental data for Udimet 700, thus verifying the characteristic relationship among the parameters under such loading paths for this material.

The investigation was extended to conditions common to cyclic tension situations in which rapid load changes occur. It is well known that the parametric relationships under cyclic loading are poorly represented by the corresponding monotonically determined relationship. Therefore, a simple method was sought by which to modify the hodograph in order to account for the effects of cyclic loading. The approach taken was the same as that for noncyclic conditions. Stress-strain tests were conducted with a discrete variation of the strain rate, to determine the nature of the modifications thereby caused to the hodograph. Preliminary results of a number of cyclic tests in tension were compared with response predicted by the suggested method. For comparison, the theories often used for analyzing creep flow problems, such as the strain-hardening, time-hardening, and life-fraction rules, are discussed in the light of the strain-rate approach.

The material used in the study was Udimet 700. Tests were conducted primarily at a temperature of 925° C. Additional data for other temperatures are given in the appendix.

SYMBOLS

E modulus of elasticity

t time

ϵ true strain

$\dot{\epsilon}$ strain rate

σ true stress

Φ state function

Subscripts:

creep	time-dependent flow
f	fracture
i	inelastic
p	time-independent flow
tot	total stress change
$\Delta\sigma$	stress change

HYDOGRAPHIC REPRESENTATION OF MECHANICAL EQUATION OF STATE

A relation often used to represent the so-called mechanical equation of state at a given constant temperature may be expressed in the form

$$\Phi(\dot{\epsilon}_i, \epsilon_i, \sigma) = 0 \tag{1}$$

Experimental investigations of equation (1) in the past have usually been concerned with the stress-strain-time relations obtained upon integrating the equation. The influence of strain rate has not been systematically studied.

The form of the function $\Phi(\dot{\epsilon}_i, \epsilon_i, \sigma)$ can be ascertained directly from a stress-strain test performed at a constant strain rate throughout. In this way characteristic plots of true stress against true strain for various strain rates are obtained, as in figure 2. This type of strength test permits stress to develop at a rate compatible with the imposed strain-rate condition and the characteristic rates of deformation processes of the material.

These and related characteristics are more easily evaluated if the curves of figure 2 are replotted as inelastic strain rate against inelastic strain, with stress as a discrete parameter, as in figure 3. This form of data presentation, herein termed the "characteristic hodograph" of the material, was devised (refs. 9 and 10) for study of various aspects of creep. It was also used as a theoretical model for strain-rate-dependent plastic deformation (ref. 11). At low values of strain the characteristic curves in figure 3 tend to be horizontal. This shows that for a given strain rate there is a corresponding stress at which flow can be initiated. At high strains the characteristic curves become relatively steep. Between these extremes of strain the characteristic curves pass through a minimum, which indicates a maximum stress for a given constant strain rate, or conversely, a minimum strain rate for a given constant stress.

Although the hodograph was constructed from stress-strain data, it demonstrates the features of other rate-controlled mechanical tests. Such tests include creep and stress relaxation, as well as combinations of these.

Creep Test

First to be discussed with the aid of figure 3 is the creep test. At the beginning of a creep test the specimen is loaded at a given strain rate, along line A'A; and when point A is reached, the true stress (e.g., 350 MN/m^2) is held constant. The creep response is then defined by the characteristic line ABC. At constant stress the strain rate begins to fall from the value maintained during loading and reaches a minimum at B as the creep strain increases along line AB. The region of minimum strain rate is commonly called the secondary creep region. Thereafter, the strain rate again increases as rupture is approached at C. If the test is conducted under constant load instead of constant stress, it is represented by the dashed line AB'C on the hodograph.

The creep response may be calculated from the hodograph by computing the elapsed creep time t from the equation

$$dt = \frac{d\epsilon_i}{\dot{\epsilon}_i} \tag{2}$$

It is clear from the foregoing that the initial creep rate depends on, and is in fact equal to, the inelastic strain rate during loading.

Stress Relaxation

Another rate-controlled phenomenon which can be represented in figure 3 is stress relaxation, represented by line AD. In a given stress-relaxation test the specimen is loaded to point A, after which the total strain rate $\dot{\epsilon}_{tot}$ is reduced to zero so that the total strain ϵ_{tot} remains constant. However, since only the total strain is controlled, the inelastic strain rate $\dot{\epsilon}_i$ is not reduced instantaneously to zero and, in fact, will continue to have finite values dictated by the material characteristics as described by figure 3. Thus, at the end of the loading phase the inelastic strain rate will have the characteristic value of point A. This $\dot{\epsilon}_i$ will result in a creep strain equal to $d\epsilon_i$, which in turn will be offset by an elastic strain $-d\sigma/E$, where E is the modulus of elasticity, so

that the test conditions will be satisfied, with a concomitant reduction in stress. The process continues along AD, which is governed by the formula

$$d\epsilon_i = -\frac{d\sigma}{E} \tag{3}$$

in conjunction with equation (2).

Equal-Damage Assumption

A third process of interest is one which results in the maximum rate of loading still compatible with the monotonic material flow characteristics. This rate of loading entails zero damage to the material during load buildup. A material-related damage criterion is therefore required. Both time and cycle number have been used in the past as measures of damage, but their value as fundamental criteria is questionable because neither is a materials parameter. Of the three materials parameters in the hodograph (strain rate, strain, and stress) accumulated inelastic strain appears to be the best gage of the amount of damage in the material. Since the fracture strain may be a function of strain rate at elevated temperatures, damage was taken in the present study to be the inelastic strain ϵ_i normalized with respect to fracture strain ϵ_f. Thus, for two strain rates, $\dot{\epsilon}_1$ and $\dot{\epsilon}_2$, equal damage is determined by

$$\left(\frac{\epsilon}{\epsilon_f}\right)_{\dot{\epsilon}_1} = \left(\frac{\epsilon}{\epsilon_f}\right)_{\dot{\epsilon}_2} \tag{4}$$

Such an equal-damage line is depicted in figure 3 as the line AE. Greater loading rates (to the left of AE) are assumed to be incompatible with the monotonic characteristic state of the material, since this would entail negative damage, or healing. Unloading rates greater than the natural rate of stress relaxation (to the left of AD) are also incompatible with the monotonic rate-controlled state of the material. Thus, the line EAD defines the bounds of all processes which can take place within the possibilities of the rate-controlled state of the material at point A. Any load or strain path which proceeds continuously to the right of line EAD, whether monotonic or cyclic, is assumed compatible with the material characteristics and can be determined from the curves in figure 3.

Cyclic Loading Conditions

Unfortunately, many cyclic tension loading paths, such as depicted in figure 1, occur at rates which violate the bounds of the rate-controlled process as described in the preceding section. Increase in stress is generally achieved at strain rates higher than those characteristic of the lower stresses in the cycle, and often also higher than characteristic strain rates at the maximum stress. Reversal of strain can only occur if compressive stresses are developed. Both of these situations involve discrete changes in strain rate, and both are therefore incompatible with the mechanical state conditions described by figure 3. Modifications to the hodograph are required in order to account for the large changes in strain rate which occur in cyclic problems. This can be done with the aid of monotonic tests along with modifications in the use of the hodograph as discussed in the section Prediction of Cyclic Tensile Creep.

TEST SPECIMEN, EQUIPMENT, AND PROCEDURE

Details concerning the type of test specimens, the low-cycle fatigue servocontrolled test facility, and general procedure have been adequately reported in reference 12. The form of specimen used in this investigation was the tubular hourglass shape shown in figure 1(d) of reference 12. The Udimet 700 material of which the specimens were made was heat treated as follows: 1162° C for 4 hours plus 1080° C for 4 hours plus 843° C for 4 hours plus 760° C for 16 hours, with forced-air cooling after each phase.

The material was tested at 925° C, with a 30-minute soak at temperature before application of load. The range of strain rates applied during stress-strain tests was from 6×10^{-5} per minute to 0.10 per minute. Tests performed in order to substantiate the characteristic hodograph included creep and relaxation tests and equal-damage loading, as well as combinations of these. Stress-strain tests under varying strain rates included a single increase or decrease of a factor of 10 in strain rate. Cyclic tensile creep tests were conducted under nominal maximum and minimum stresses of 450 and 310 MN/m^2, respectively. Tests were performed with both high and low initial stress, and the strain rates used during change in stress were 0.04 per minute and 0.005 per minute.

RESULTS AND DISCUSSION

Experimental results are presented in two sections. First, data obtained in constant-strain-rate tensile tests are presented in conventional form and as the corresponding hodograph, and results of tests conducted along various loading paths are

compared with response predicted with the aid of the characteristic hodograph. Secondly, results obtained from stress-strain tests with varying strain rate and from cyclic tests are presented and discussed.

Stress-Strain Tests at Constant Strain Rate

True-stress - true-strain curves obtained at 925° C from Udimet 700 material under constant strain rates are shown in figure 2, and the hodograph in figure 3.

The stress-strain curves shown in figure 2 are strongly dependent on strain rate, and the material response is primarily due to time-dependent (creep) flow. Proportional limit, maximum true stress, and failure strain all increase with increasing strain rate. The maximum stress is developed fairly early in the test, occurring at a true strain of 0.02 at a low strain rate (5×10^{-5}/min) and at 0.06 at the highest strain rate employed (0.1/min). Beyond the point of maximum stress the curves slope off gradually until shortly before failure, when they drop steeply to the fracture point. The appearance of reduction in stress on true-stress - true-strain curves at elevated temperatures indicates that the deformation is governed by the time-dependent (creep) mechanism. Note that the maximum stresses, the dropoff points, and the fracture points appear to lie respectively on straight lines radiating from the origin of the stress-strain curves. This is consistent with an observation made previously in reference 8. The characteristic hodograph is shown in figure 3. Its essential features have already been discussed.

A detailed discussion of the observed yield behavior and ductility of the material appears in the appendix. The report is limited here to presentation of results pertaining to the use of the characteristic hodograph for predicting material response to various loading paths.

Comparison with Predicted Creep and Relaxation Response

A number of tests were conducted under conditions of constant-load creep and stress relaxation, and combinations of these, in order to compare experimental results with behavior predicted by use of the characteristic hodograph. The duration of the tests varied from 0.06 to 11.3 hours.

Results of two constant-load creep tests are compared with calculated results in figure 4. Figures 4(a) and (b) are for creep under initial true stresses of 425 and 320 MN/m^2, respectively. The predicted creep curves (dashed line) are in fairly good agreement with experimental data (solid line), and calculated and actual rupture times agree within one-third of a decade.

Stress-relaxation results are shown in figure 5. The predicted stress-relaxation curve for the first cycle lies within 3 percent of the experimental curve. Test results involving a constant-strain-rate loadup followed by stress relaxation, which was in turn followed by a constant-load creep runout to rupture, are shown in figure 6. Creep stress was equal to the stress at the end of the relaxation phase, and agreement between predicted and experimental results is very good.

Finally, a test was conducted (fig. 7) which consisted of a constant-strain-rate loadup, followed by a stress-relaxation phase, an equal-damage reload, and a creep runout to rupture. The reloading phase along an equal-damage line was carried out in accordance with equation (4). The calculated curves are again in close agreement with test data, in spite of the complex nature of the test.

To conclude this section it appears that the hodograph constructed from constant-strain-rate stress-strain data can be used successfully for predicting time-dependent material behavior of Udimet 700 at 925° C when changes in strain rate do not occur instantaneously. This result concurs with results for other materials and longer times in references 5 and 8. The relationship between the monotonic hodograph and material response to sudden changes in strain rate is discussed next.

Stress-Strain Tests at Two Strain Rates

Results of stress-strain tests with a single, stepwise decrease or increase in strain rate are shown in figures 8 and 9, respectively. In each case the test was initiated at a given strain rate, and at some inelastic strain the rate of straining was increased or decreased approximately tenfold. After a decrease in strain rate (fig. 8), the material responded as if the lower strain rate had been applied from the outset and continued along the original stress-strain curve at this strain rate. This behavior was to be expected because the reduction in stress which occurred immediately after the change in strain rate was governed by conditions similar to those obtained during stress relaxation, although in this case the total strain was permitted to increase during the stress reduction. It has been shown previously (figs. 5 to 7) that the more critical case of stress relaxation is compatible with the characteristic hodograph. The same should be true, therefore, when the strain rate is reduced but still positive. Note that the prestrain at high strain rate somewhat strengthens the material at large strains at the lower strain rate, although ductility is slightly reduced.

The increase in stress developed after a discrete increase in strain rate (fig. 9) was insufficient to reach the stress-strain curve of the virgin material (without prestrain). When the change occurred in the primary or early secondary stage (approximately 4 percent inelastic strain or less), elastic stress-strain response recurred until the stress reached the proportional limit stress of the virgin material. At this point inelastic

strain began to accumulate again. The subsequent curves were rather flat, and little or no strain hardening occurred. The stress remained in the region of the initial proportional limit stress until the fairly sudden dropoff before failure occurred. Total elongation was about 25 percent less than for the virgin material. When the material was prestrained beyond the point of maximum true stress (approximately 6 percent inelastic strain, as seen in fig. 9(a)), the subsequent stress developed was lower than the initial proportional limit. This was probably due to the fact that the mechanism which would eventually lead to failure had already been initiated during prestraining at the low strain rate.

These data indicate the manner in which the hodograph is altered if a discrete change in strain rate occurs in a test. For a decrease in strain rate the process is compatible with the hodograph as defined heretofore. For an increase in strain rate the primary creep mechanism is reactivated, and the hodographic curve is raised. The constant-stress curve for the increased strain rate starts at the level corresponding to the original flow stress for that strain rate, but it does not dip downwards as strain is accumulated. Instead it remains essentially horizontal until third-stage creep is reached, after which it again follows the original hodograph until failure occurs.

Prediction of Cyclic Tensile Creep

In the light of the material response to discrete changes in strain rate, a simple method was devised for estimating time-dependent flow behavior under cyclic tensile loading conditions. The method is based on the following guidelines:

(1) For loading that increases faster than the equal-damage rate, the stress and the strain rate reached are taken to be equal to the flow stress and the corresponding primary strain rate, as given by the hodograph. If either stress or strain rate is maintained, the other will remain at the corresponding primary-stage level until third-stage strains are developed. Thereafter, the failure mechanism will operate as in a monotonic test or process.

(2) In all other cases, with the exception of forced (compressive) unloading, the hodograph is assumed to govern the material response.

A number of preliminary cyclic tests were conducted in order to test the proposed method of calculation. Results of a repeated stress-relaxation test are presented in figure 10 and compared with predictions made by the preceding method. The test included three reloads, which were carried out at high rate so that negligible additional inelastic deformation occurred during reload; that is, reload occurred along a vertical path on the hodograph. (This path represents the so-called strain-hardening theory and lies to the left of the assumed equal-damage line.) The first cycle was shown previously in figure 5. Agreement between prediction and experiment in the three later cycles was

almost as good as in the first cycle, as can be seen from figure 10. The strain-hardening rule would predict lower strain rates and, therefore, somewhat higher stresses.

Four cyclic creep tests were performed, and the results are shown in figure 11 in hodographic form. The characteristic curves for 450 and 310 MN/m^2 as obtained from controlled-strain-rate tensile tests (fig. 3) have been added for the sake of reference. The cyclic creep data are represented by dashed lines, and the modified hodographic line for the reference maximum stress of 450 MN/m^2 used appears as a small-dashed line. At the minimum stress the data lie close to the corresponding hodographic curve as predicted. The strain rate at the maximum stress remained on the level of the primary strain rate for that stress, until an inelastic strain of approximately 0.08 was accumulated (figs. 11(a) to (d)), after which the data tended to follow the third-stage portion of the characteristic curve. Thus, the data obtained appear to substantiate the proposed method of prediction.

In the two tests, the strain rate during stress change $\dot{\epsilon}_{\Delta\sigma}$ was equal to 0.005 per minute, which was the minimum creep rate for the maximum stress applied (figs. 11(c) and (d)). Under such conditions the monotonic hodograph should have accumulated considerable inelastic strain during the first reload and continued to strain at the minimum rate corresponding to the maximum stress. However, a negligible amount of inelastic strain occurred during each reload, and the material flowed at a higher rate when the maximum stress was reached. The explanation is that although the strain rate during load change was relatively low, corresponding to the second-stage strain rate at the higher stresses in the cycle, it was higher than the normal strain rates at the lower cyclic stresses. Thus, the response over a large portion of the stress rise is elastic, so that the maximum stress was reached with the material in a strain-hardened condition and the primary strain rate was reactivated.

Cyclic creep lifetimes calculated for the tests are compared with experimental results in figure 12. Also included in the figure (circular symbols) are results of previous monotonic creep tests (figs. 4, 6, and 7), as well as three tests (square symbols) consisting of stress relaxation followed by rapid increase or decrease in stress and runout to failure at constant load. Cyclic creep results are shown as triangular symbols. Although the present tests did not cover a large time range, the good agreement shown in figure 12 is very promising.

Comparison with Other Theories for Cyclic Creep

The cyclic loading path is, of course, not new; and a number of theories have been advanced in the past for describing creep behavior subsequent to a sudden change in stress. Well known among them are the time-hardening, strain-hardening, and life-

fraction rules (ref. 13). These theories may be conveniently compared in figure 13 with the method proposed herein with the aid of the hodographs.

According to the time-hardening rule, the creep behavior of a material at any stress level depends on the value of stress and the total time elapsed since the beginning of the creep process. Change of stress is achieved along lines of constant time, which are represented in accordance with equation (2) at 45° to the horizontal on the hodograph (AB' in fig. 13). Thus, a rapid increase in stress at point A in figure 13(a) will result in a moderate rise in strain rate to point B'. The material will continue to creep along the curve designated "time hardening" in the figure, from the point B defined by the creep strain at A and the strain rate at B'. A rapid decrease in stress will result in a moderate drop in strain rate from point A in figure 13(b) to point B'. The subsequent creep curve begins at B (fig. 13(b)) defined as before. Once the end of the so-called secondary creep stage has been reached, a stress increase apparently cannot be accomplished along a line of constant time, since the hodograph indicates decreasing stresses in this region.

The strain-hardening rule states that material would respond to a change in creep stress as if the change were achieved at constant inelastic strain. It does not take into account the effect of strain rates obtaining during the stress change. The strain-hardening rule is represented in figures 13(a) and (b) by the vertical line AC. The creep curve follows the monotonic hodographic curve for the new stress from point C, whether the stress was increased or decreased.

From figure 13 it is clear that the strain-hardening rule predicts higher strain rates than does the time-hardening rule when stress is increased in the primary stage or decreased in the third stage. The strain-hardening rule predicts lower strain rates when stress is decreased in the primary stage or increased in the third stage. If the applied loading is cycled a number of times before failure occurs, these opposing effects will tend to cancel each other, and predictions made in accordance with the time-hardening and strain-hardening rules will converge on each other.

The life-fraction rule states that the damage occurring in a material is a function of the fraction of rupture time which has been consumed. Although the life-fraction rule was conceived as a criterion for rupture life, it has been applied to the calculation of flow behavior. In the interest of clarity the life-fraction rule is not depicted in figure 13. However, it generally falls between the time-hardening and strain-hardening rules on the line BC, and proceeds between the two dashed curves. It has been shown (ref. 14) that the life-fraction and strain-hardening rules coincide when the total elongation at fracture is constant and independent of strain rate. Under this condition a given inelastic strain (strain-hardening rule) corresponds to a fraction of rupture time which is constant at any level of strain rate or stress (life fraction). The equal-damage concept proposed in the present report and defined by equation (4) is vertical in this case, coincident with the strain-hardening and life-fraction rules. The equal-damage concept can therefore be considered as a ductility-fraction rule.

The method suggested herein for predicting cyclic creep flow is also represented in figure 13. For reduction in stress the proposed method coincides with the strain-hardening rule. For an increase in stress the method predicts a strain rate which is considerably higher than that predicted by the other theories discussed. In the latter case the resulting failure time can be from 3 to 8 times less than predicted by the other theories.

SUMMARY OF RESULTS

A study was made of the significance of strain rate in the prediction of uniaxial inelastic properties of Udimet 700 at 925° C. Tests were performed in order to investigate the feasibility of using the relationship among strain rate, strain, and stress, from strength tests, for predicting time-dependent material behavior under other loading conditions. The strain rate during these tests ranged from 6.0×10^{-5} to 0.10 per minute. Predictions of material response for a number of noncyclic loading paths were made from the characteristic tensile hodograph and were compared with test data generated. Stress-strain tests were then conducted with stepwise changes in strain rate, to determine the nature of modifications caused to the hodograph. A method, based on the monotonic hodograph, was suggested for predicting cyclic creep behavior; and results calculated by this method were compared with preliminary test data obtained.

The major results of this investigation are as follows:

1. For continuous-strain-rate tests there exists a unique relationship among inelastic strain rate, inelastic strain, and stress. This mechanical state is usefully represented in graphical form as a characteristic hodograph of the three parameters. Good agreement is obtained between experimental results and material behavior predicted from the hodograph.

2. When strain rate is discontinuous, primary creep is reactivated until the inelastic strain reaches third-stage creep magnitude. Continuous increases and all decreases in strain rate result in behavior which corresponds to the characteristic hodograph.

3. A simple method is proposed for estimating creep response under cyclic tensile stresses from the hodograph. Comparison between predicted response and results of preliminary cyclic creep tests in tension show good agreement.

Lewis Research Center,
National Aeronautics and Space Administration,
Cleveland, Ohio, June 9, 1972,
501-21.

APPENDIX - SUPPLEMENTARY MATERIALS DATA ON UDIMET 700

A number of remarks are made here with regard to features of the stress-strain data obtained at constant strain rates for Udimet 700 at various temperatures. Although most of the results were obtained at 925° C and are reported in the text, additional data taken at 760° C, 525° C, and room temperature are presented here for completeness. Topics discussed include yield phenomena such as flow stress, maximum stress, ductility, and strain energy.

Hodograph for 760° C

Stress-strain curves obtained at 760° C are shown in figure 14. These curves are similar to those at 925° C, with a number of significant differences. At strain rates below 0.1 per minute the shape of the curves is generally the same as at the higher temperature, although the effect of strain rate is not as strong. The curves are somewhat flatter, the maximum stress is developed at a higher true strain, and total elongation is higher at any given strain rate. Again the dropoff points and the fracture points tend to lie on two straight lines emanating from the origin. However, at strain rates above 0.01 per minute, a change in behavior occurs. At low inelastic strains the stress-strain curves coincide, becoming less sensitive to strain rate as the rate increases. At the failure end of the curves the stress dropoff is less and the ductility also decreases.

These features are clearly delineated in the hodograph of figure 15. At high strain rate the characteristics tend to become vertical, indicating that the strain is insensitive to strain rate. In other words, at 760° C, high strain rates engender true plastic time-independent behavior. However, as the test progresses, time-dependent effects can still enter. At a strain rate of 0.1 per minute figure 15 shows that time-dependent effects begin to occur when a stress of approximately 1275 MN/m^2 is developed. Even though part of the total inelastic strain is thus due to creep, at high strain rate the failure strain is reduced from the expected ductility and approaches the true, time-independent ductility. It would be of interest to examine how the material responds to an increase in strain rate at this temperature and how the time-dependent and time-independent deformations interact under such a loading path.

The two types of inelastic deformation discernible in the hodograph for 760° C are supported by the micrographs in figure 16. The specimens tested at moderate strain rates (0.0024/min and 0.01/min) indicate time-dependent failure, as at the higher temperature. The presence of many grain-boundary cracks and fracture lines which follow the grain boundaries is evidence of the grain-boundary flow common to the creep phenemon. On the other hand, the specimen tested at a strain rate of 0.09 per minute clearly indicates predominantly time-independent flow and fracture, as at low

temperatures. The micrograph is similar to that of the undeformed material (cf. fig. 6-2, ref. 15), except that the grains near the edges and the fracture line are plastically elongated. The 45° fracture surface is plainly transcrystalline.

Completely plastic behavior (independent of strain rate) was found at 525° C and at room temperature, as shown in figure 17. For a given temperature, essentially identical results were obtained at nominal strain rates of 0.01 and 0.0003 per minute, precluding the construction of hodographs.

Yield Phenomena

True flow stress and maximum true stress developed are shown in figure 18 as a function of strain rate for the test temperatures employed. The flow stress was taken to be the stress in the material when the inelastic strain equaled 0.0001 or more. For a given elevated temperature the dependence of flow stress and maximum stress on strain rate is linear, and the flow- and maximum-stress lines are parallel at low strain rates on the logarithmic plot of figure 18. The material behavior is more sensitive to strain rate as the test temperature rises. However, with reduction of temperature, first the flow stress and later also maximum stress become independent of strain rate. The flow stress in the range between room temperature and 760° C (at strain rates greater than 0.0015/min) is essentially constant. Such strain-rate-independent behavior indicates the transition from creep flow to true plastic flow.

Discontinuous yielding was observed in the material at each test temperature both in tension and in compression. This behavior was marked by serrations throughout the upper portion of the load-strain curves generated during tests. At high temperatures (760° and 925° C) each serration consisted of a sharp drop in load as local yielding occurred and overshot the command strain signal, followed by a gradual recovery of the load. A number of high load peaks also occurred during such tests, as a result of local strain hardening. Local strain hardening can occur at temperatures in the creep range, since the material never becomes fully strain hardened at these temperatures.

At lower test temperatures (room temperature and 525° C) strain-hardening peaks did not appear since the material sustained full strain hardening for a period of time before the next local yield occurred. At 525° C the local yielding was sudden and pronounced and was accompanied by audible thuds, in compression as well as in tension. Similar behavior was reported by Wells and Sullivan (ref. 16), who attributed it to sudden bursts of slip. Even when the hydraulic pressure was throttled down in order to minimize the large drop in load during local yielding at 525° C, at least one massive slip burst always occurred during which the load dropped to zero temporarily. The number of slip bursts occurring increased as the strain rate decreased, although at these temperatures the elongation was constant and independent of strain rate.

The slip bursts were generally spaced at random throughout the plastic portion of the stress-strain curve, the first one occurring shortly after initial yield of the material. An interesting exception was the case in which the specimen underwent appreciable time-dependent flow in compression at high temperature before being tested to fracture in tension under time-independent conditions. In this case no slip bursts appeared in tension until the inelastic creep strain imposed in compression was reversed by plastic tensile strain. This case is a marked example of strain-range partitioning, which is used in the creep-fatigue analysis of reference 1.

Ductility

Total true strain obtained at fracture in tensile strength tests is plotted against strain rate in figure 19. In general, a linear logarithmic relationship appears to hold. However, at 760° C and high strain rate, a significant drop in elongation occurs, accentuating the difference between time-independent and time-dependent mechanisms. This relatively low elongation approaches the average elongation of 0.14 obtained at temperatures below the creep regime and indicates that the failure mechanism at this strain rate is predominantly plastic shear.

In the light of these results for creep and plastic ductility, the question arises whether the ductility at lower strain rates is truly dependent on strain rate, or whether it rather consists of a combination of constant creep ductility and the plastic strain corresponding to the maximum stress achieved. This concept is illustrated in figure 20. The upper curve is the true plastic (time independent) curve, and the lower curve represents stress-strain data obtained at a strain rate $\dot{\epsilon}_2$ such that both plastic and creep strains were developed. Thus, the portion of the ductility at $\dot{\epsilon}_2$ due to plasticity is given by ϵ_p at the maximum stress of the lower curve, and the remainder is the creep ductility.

Generally, in the range of strain rates for which creep is significant, the plastic strain developed is never greater than 5 percent of the total elongation and is usually much less. Thus, the effect of the plastic component on the rate dependence of the ductility is negligible.

A number of tests were performed to determine the effect of compressive flow on subsequent tensile ductility (fig. 21). A significant difference in results was observed depending on the mechanism of compressive flow. When the compressive prestrain was carried out under conditions of creep flow (925° C) up to 29 percent strain, either by means of stress-strain or constant-load creep, the tensile ductility resulting was of the same order of magnitude as that obtained without prestraining in compression. This was so when the mode of tensile failure was creep (925° C). However, when failure occurred by plastic shear (525° C), the ductility was actually increased by approximately the amount of prior compressive creep flow. On the other hand, when the prestraining

entailed compressive plastic flow (525° C) of the order of 12 percent, subsequent tensile creep elongation at 925° C was less than one-half the original elongation. Plastic ductility (at 525° C) was reduced somewhat by prior compressive plastic flow but remained of the same order as that of virgin material.

It appears, on the one hand, therefore, that creep prestrain in compression has little effect on tensile creep ductility and that plastic prestrain in compression has little effect on tensile plastic ductility for Udimet 700. On the other hand, compressive plastic prestrain causes a significant reduction in tensile creep ductility, and compressive creep prestrain causes a complementary increase in tensile plastic ductility.

Strain Energy

Strain energy to failure in tension was measured as the area under the true tensile stress-strain curve. Results shown in figure 22 indicate a linear logarithmic relationship for the range of strain rate in which the strain energy is variable. At high strain rates, plastic behavior of the material is evidenced by a leveling off at a constant value of strain energy. This can be seen from the 760° C curve in the figure, but strain rates at 925° C were insufficient to preclude time-dependent behavior.

Prior compressive strain at 925° C had no effect on the subsequent tensile strain energy at that temperature. This result is in agreement with elongation data discussed in the previous section.

REFERENCES

1. Manson, S. S.; Halford, G. R.; and Hirschberg, M. H.: Creep-Fatigue Analysis by Strain-Range Partitioning. Symposium on Design for Elevated Temperature Environment. ASME, 1971, pp. 12-28.

2. Manson, S. S.; and Halford, G. R.: A Method of Estimating High-Temperature, Low-Cycle Fatigue Behavior of Materials. Proceedings of the International Conference on Thermal and High-Strain Fatigue. Metals and Metallurgy Trust, London, 1967, pp. 154-170.

3. Spera, David A.: The Calculation of Elevated-Temperature Cyclic Life Considering Low-Cycle Fatigue and Creep. NASA TN D-5317, 1969.

4. Manson, S. S.; Halford, G. R.; and Spera, D. A.: The Role of Creep in High Temperature Low Cycle Fatigue. Advances in Creep Design. A. I. Smith and A. M. Nicolson, eds., Applied Science Publishers, Ltd., 1971, pp. 229-249.

5. Lubahn, J. D.; and Felgar, R. P.: Plasticity and Creep of Metals. John Wiley & Sons, Inc., 1961.

6. Ludwik, P.: Elements of Engineering Mechanics. Springer, Berlin, 1909.

7. Hollomon, J. H.: The Mechanical Equation of State. Trans. AIME, vol. 171, 1947, pp. 535-543.

8. Nádai, Arpád: Theory of Flow and Fracture of Solids. Vol. II. McGraw-Hill Book Co., Inc., 1963.

9. Glen, J.: A New Approach to the Problem of Creep. J. Iron Steel Inst., vol. 189, pt. 4, Aug. 1958, pp. 333-343.

10. Glen, J.: Ductility in High-Temperature Rupture Tests. J. Iron Steel Inst., vol. 190, pt. 1, Sept. 1958, pp. 30-39.

11. Hart, E. W.: A Phenomenological Theory for Plastic Deformation of Polycrystalline Metals. Acta Met., vol. 18, no. 6, June 1970, pp. 599-610.

12. Hirschberg, M. H.: A Low Cycle Fatigue Testing Facility. Manual on Low Cycle Fatigue Testing. Spec. Tech. Publ. 465, ASTM, 1969, pp. 67-86.

13. Mendelson, A.; Hirschberg, M. H.; and Manson, S. S.: A General Approach to the Practical Solution of Creep Problems. J. Basic Eng., vol. 81, no. 4, Dec. 1959, pp. 585-598.

14. Berkovits, Avraham: Investigation of Three Analytical Hypotheses for Determining Material Creep Behavior Under Varied Loads, with an Application to 2024-T3 Aluminum-Alloy Sheet in Tension at 400° F. NASA TN D-799, 1961.

15. Blankenship, Charles P.: Thermomechanical Processing of the Nickel-Base Alloy U-700. Aerospace Structural Materials. NASA SP-227, 1970, pp. 91-100.

16. Wells, C. H.; and Sullivan, C. P.: The Effect of Temperature on the Low-Cycle Fatigue Behavior of Udimet 700. Trans. ASM, vol. 60, no. 2, June 1967, pp. 217-222.

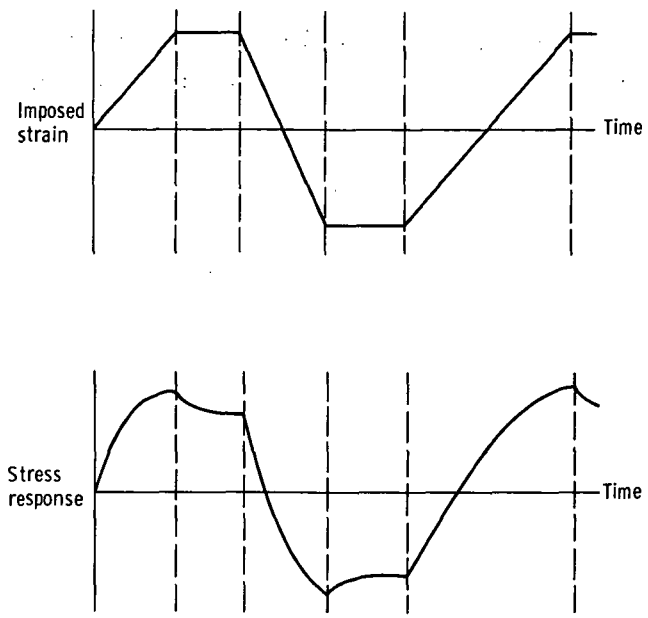

Figure 1. - Example of strain cycle at elevated temperature.

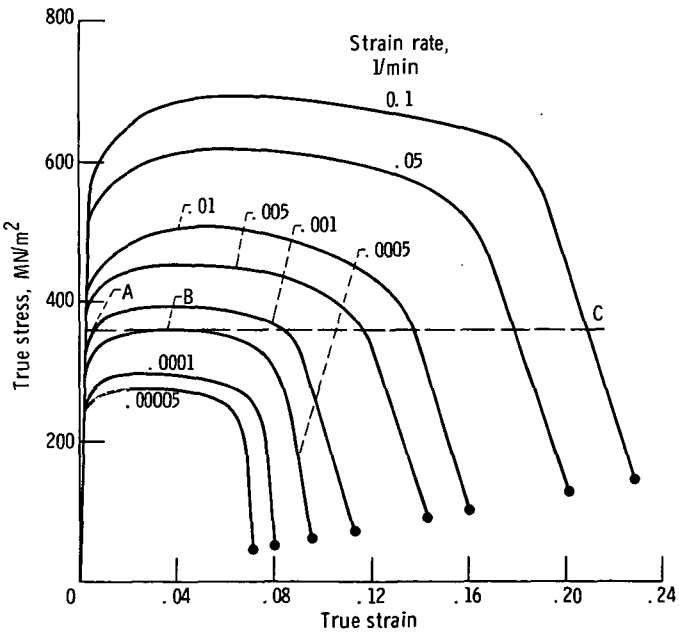

Figure 2. - Tensile stress-strain properties of Udimet 700 at 925° C.

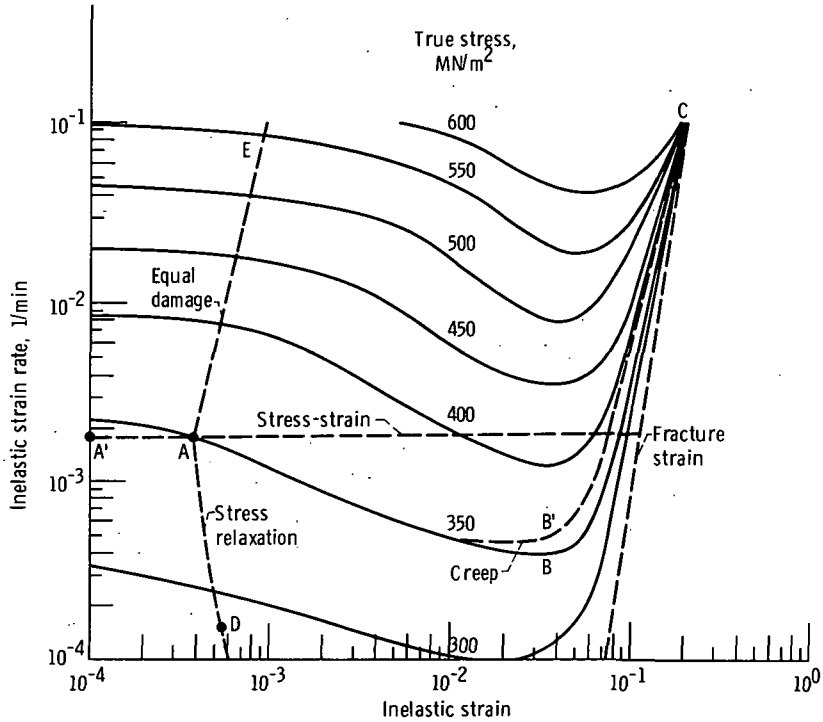

Figure 3. - Hodograph for Udimet 700 in tension at 925° C.

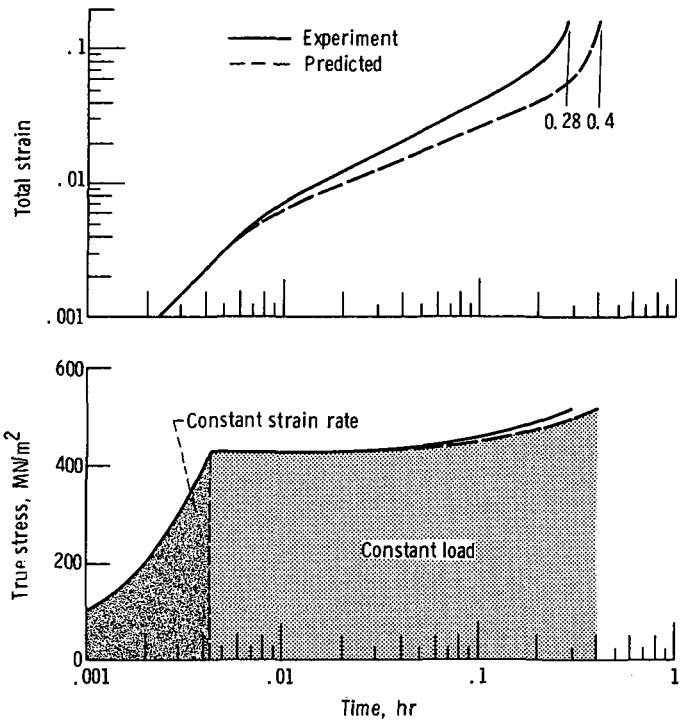

(a) Initial true stress, 425 MN/m^2.

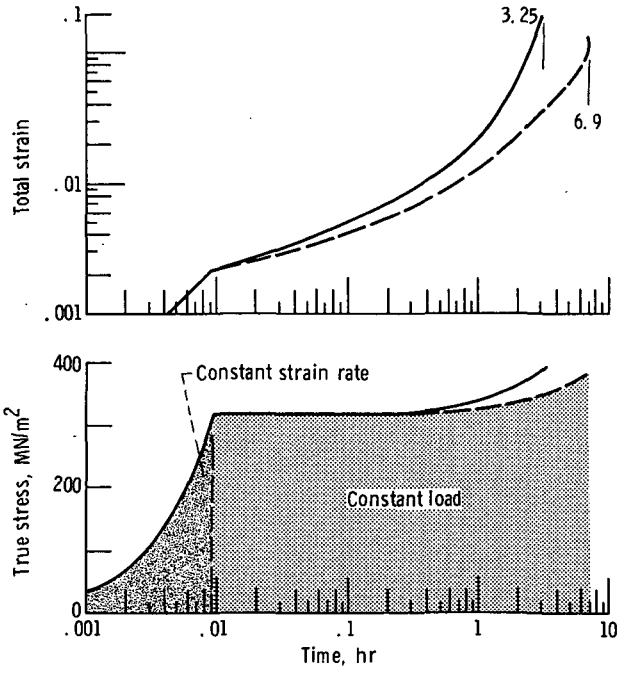

(b) Initial true stress, 320 MN/m^2.

Figure 4. - Creep of Udimet 700 under constant load at 925° C.

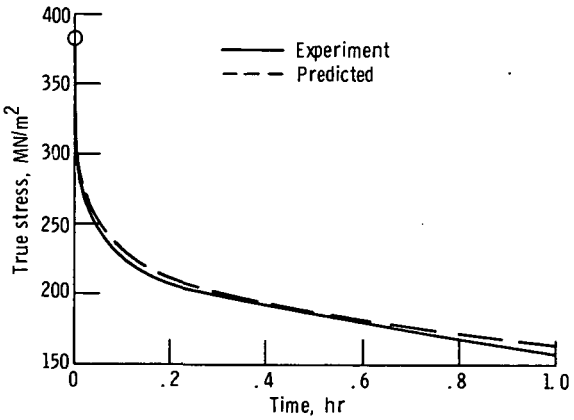

Figure 5. - Stress relaxation of Udimet 700 at 925° C. Initial stress, 380 MN/m^2; loading strain rate, 0.0045 per minute.

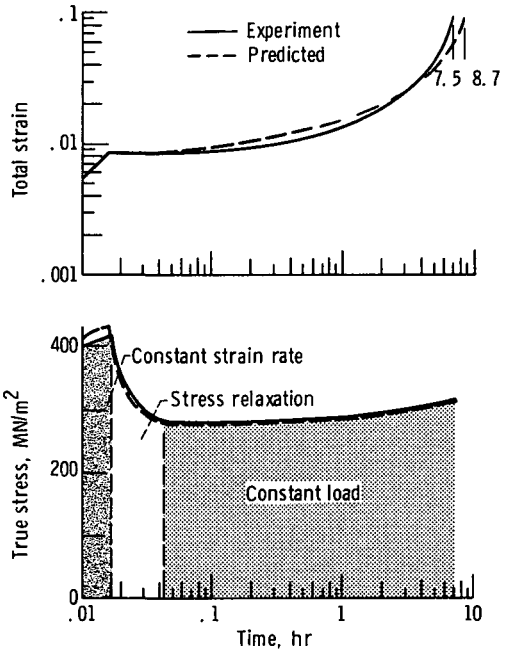

Figure 6. - Stress relaxation followed by creep for Udimet 700 at 925° C.

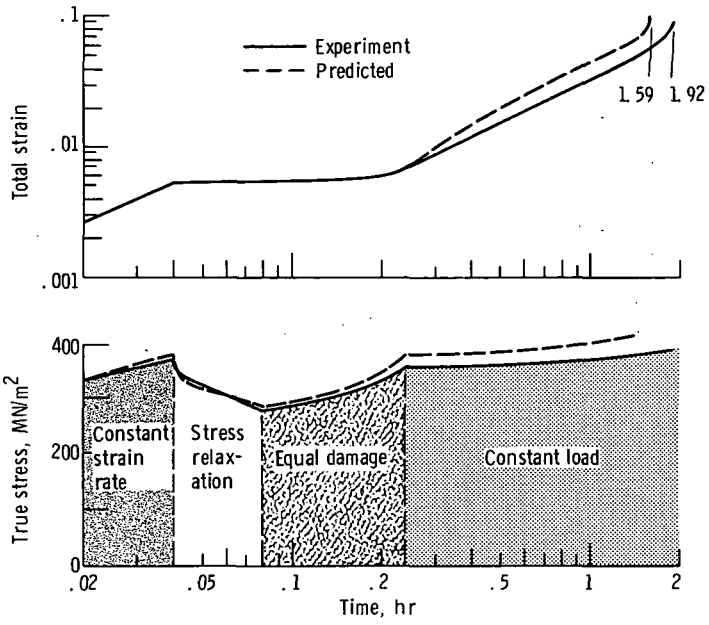

Figure 7. - Stress relaxation followed by equal-damage reload and creep for Udimet 700 at 925° C.

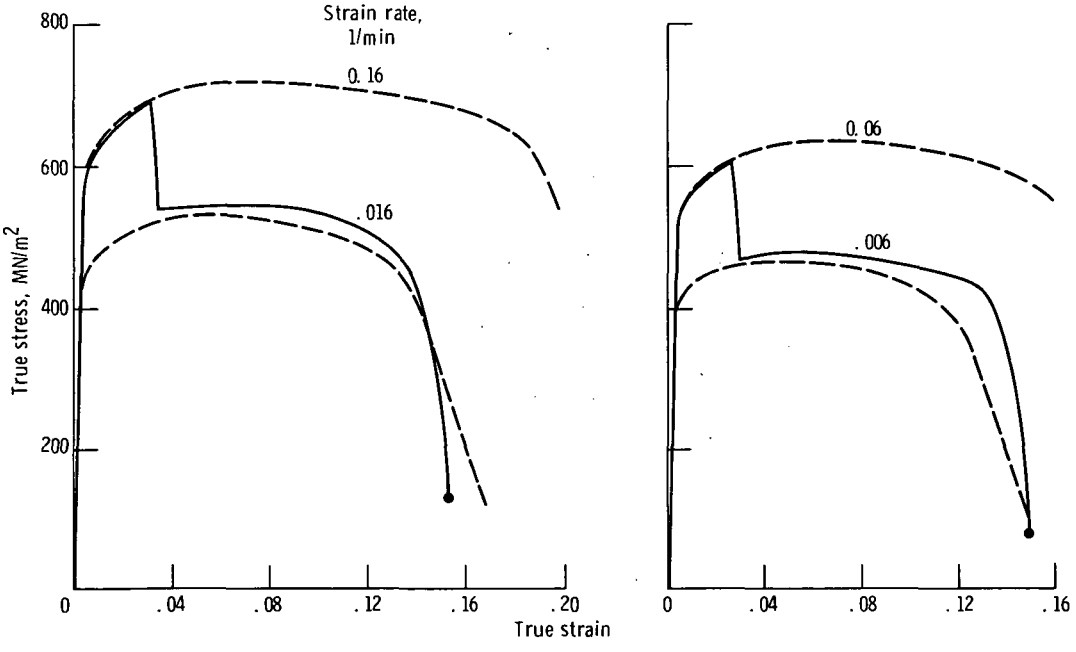

Figure 8. - Decrease in strain rate for Udimet 700 at 925° C.

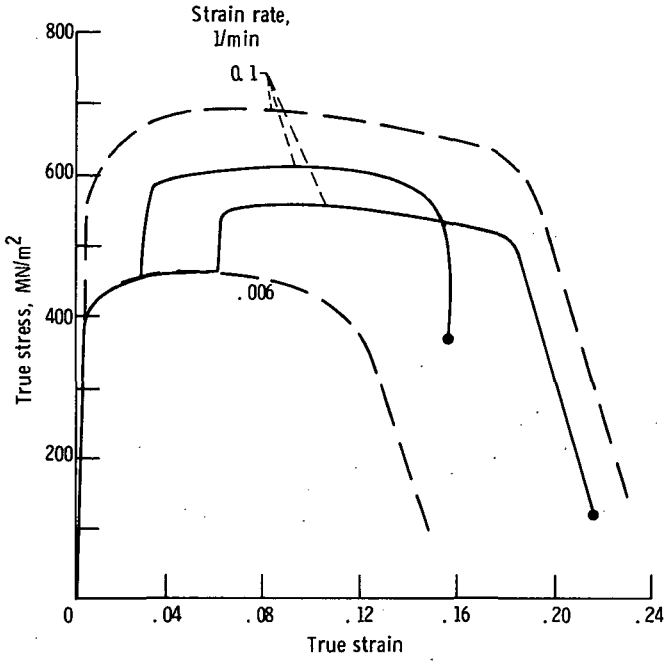

(a) Strain rate increased from 0.006 per minute to 0.10 per minute.

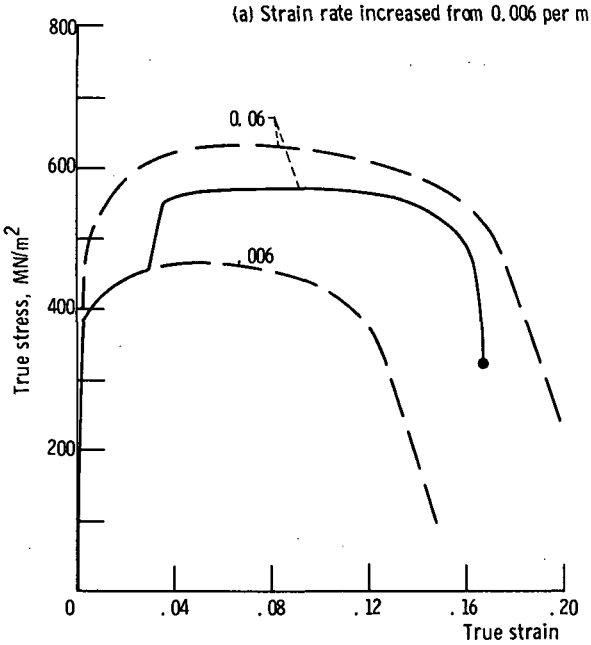

(b) Strain rate increased from 0.006 per minute to 0.06 per minute.

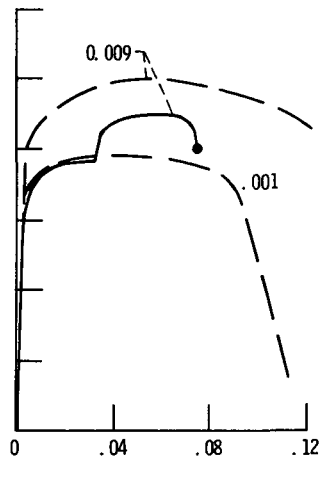

(c) Strain rate increased from 0.001 per minute to 0.009 per minute.

Figure 9. - Increase in strain rate for Udimet 700 at 925° C.

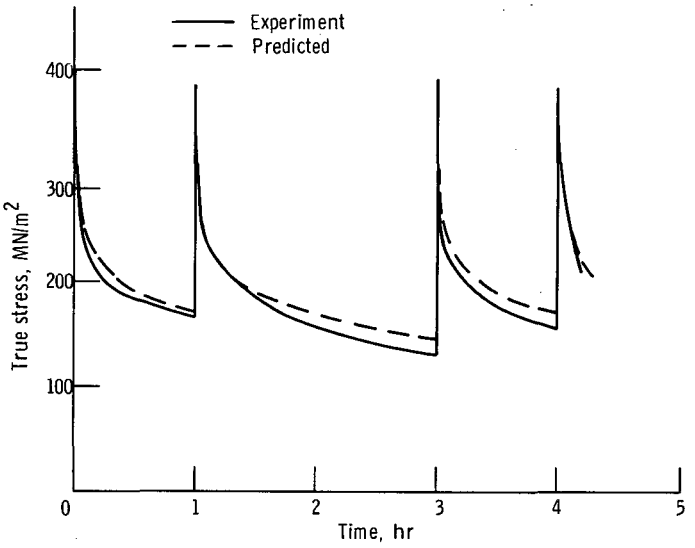

Figure 10. - Repeated stress relaxation of Udimet 700 at 925^0 C.

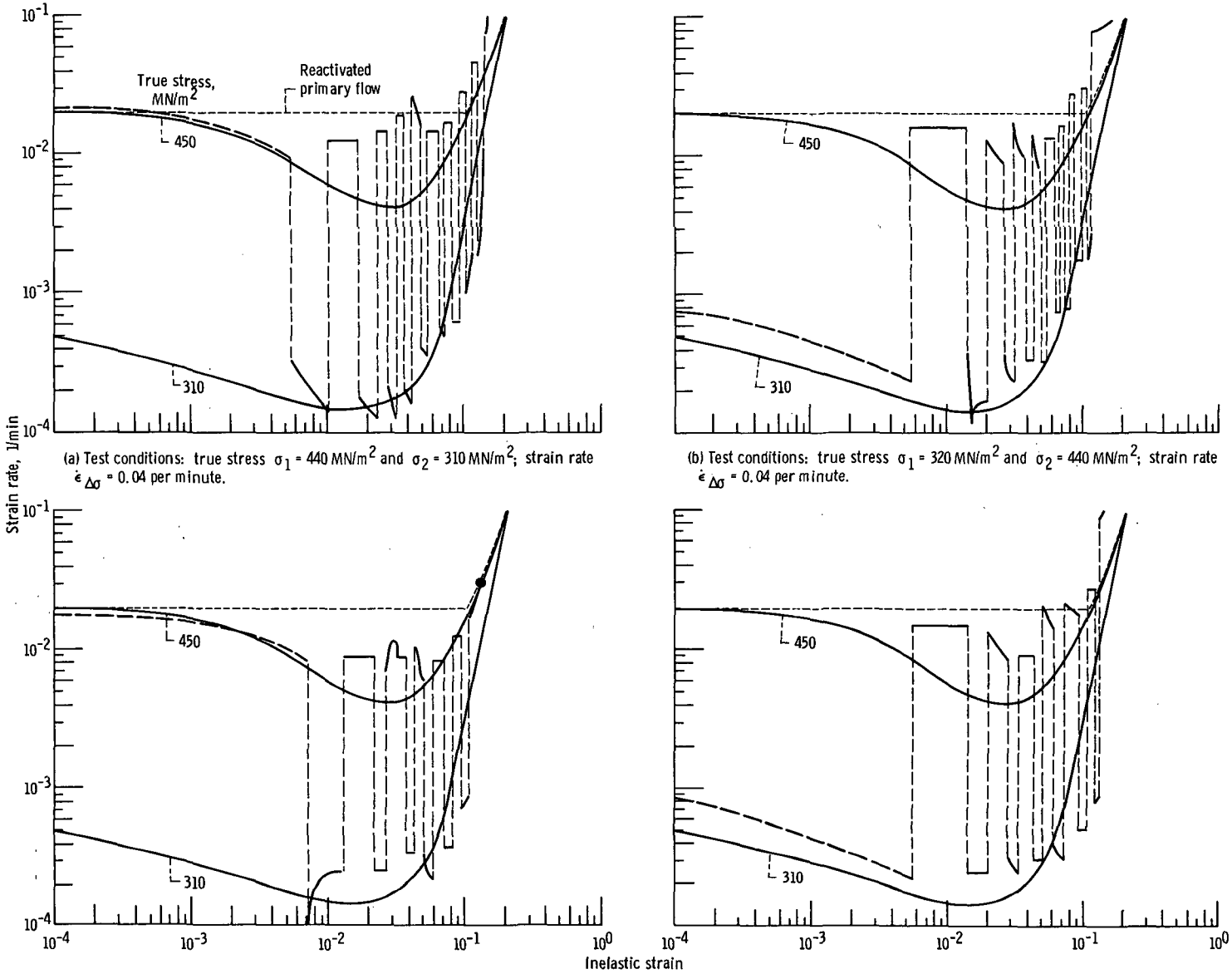

(a) Test conditions: true stress σ_1 = 440 MN/m^2 and σ_2 = 310 MN/m^2; strain rate $\dot{\epsilon}_{\Delta\sigma}$ = 0.04 per minute.

(b) Test conditions: true stress σ_1 = 320 MN/m^2 and σ_2 = 440 MN/m^2; strain rate $\dot{\epsilon}_{\Delta\sigma}$ = 0.04 per minute.

(c) Test conditions: true stress σ_1 = 450 MN/m^2 and σ_2 = 320 MN/m^2; strain rate $\dot{\epsilon}_{\Delta\sigma}$ = 0.005 per minute.

(d) Test conditions: true stress σ_1 = 315 MN/m^2 and σ_2 = 450 MN/m^2; strain rate $\dot{\epsilon}_{\Delta\sigma}$ = 0.005 per minute.

Figure 11. - Cyclic tensile creep of Udimet 700 at 925° C.

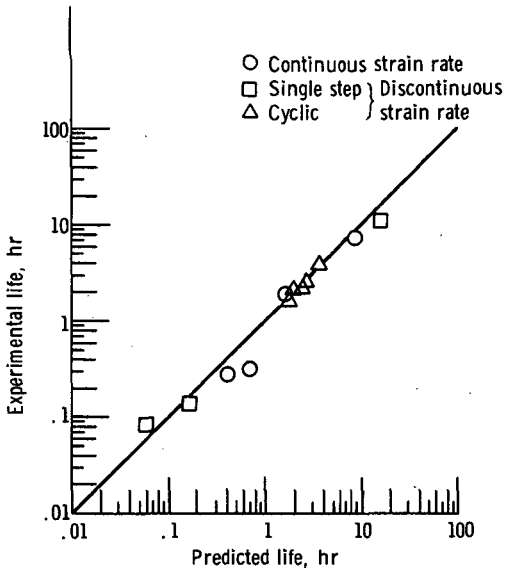

Figure 12. - Creep failure of Udimet 700 at 925° C.

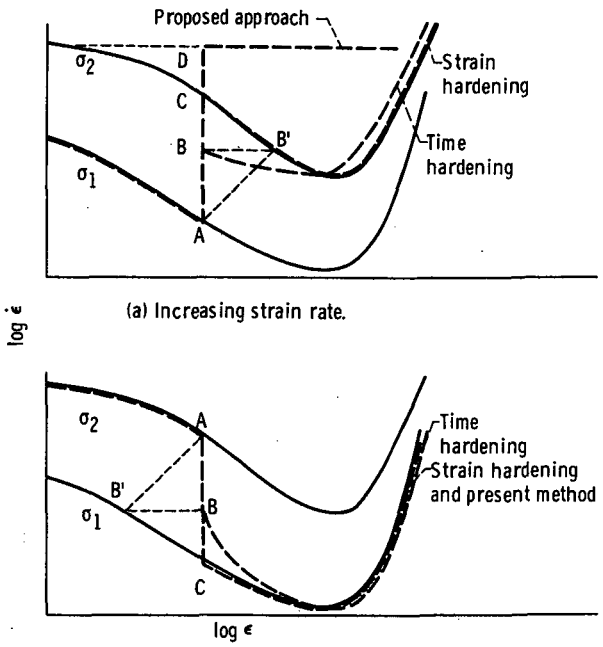

Figure 13. - Comparison between cyclic creep theories.

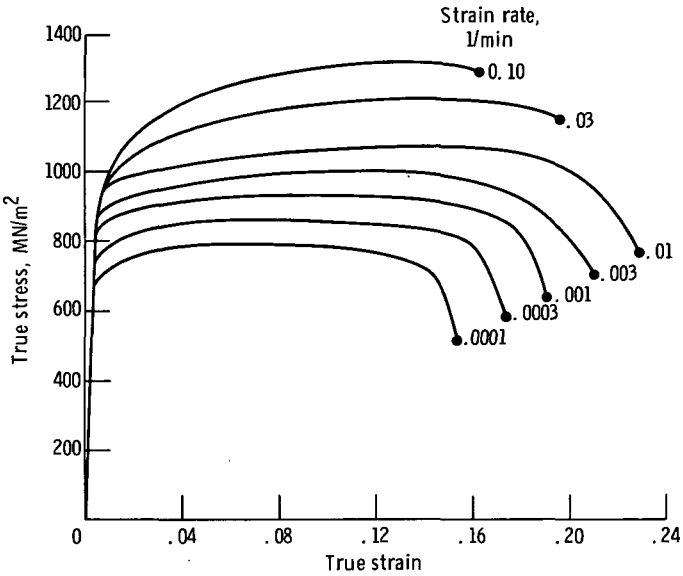

Figure 14. - Tensile stress-strain properties of Udimet 700 at 760° C.

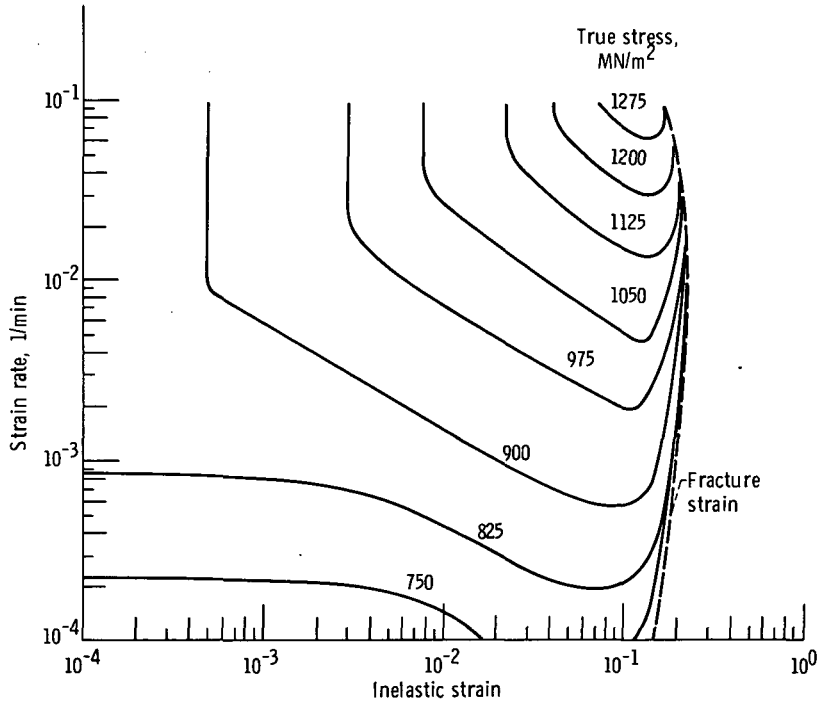

Figure 15. - Hodograph for Udimet 700 in tension at 760° C.

Strain rate, 0.0024 per minute

Strain rate, 0.01 per minute

CS-61429

Strain rate, 0.09 per minute

Figure 16. - Failures resulting from constant-strain-rate tests of Udimet 700 at 760° C.

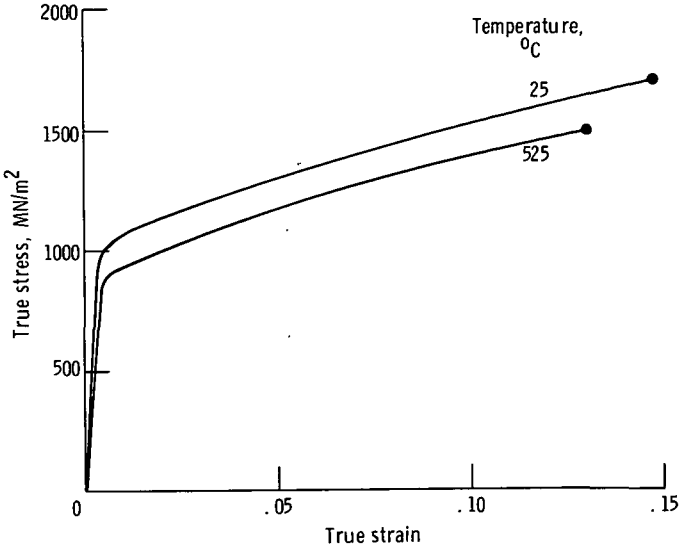

Figure 17. - Tensile stress-strain properties of Udimet 700 at room temperature and 525^0 C ($10^{-4} < \dot{\epsilon} < 10^{-2}$).

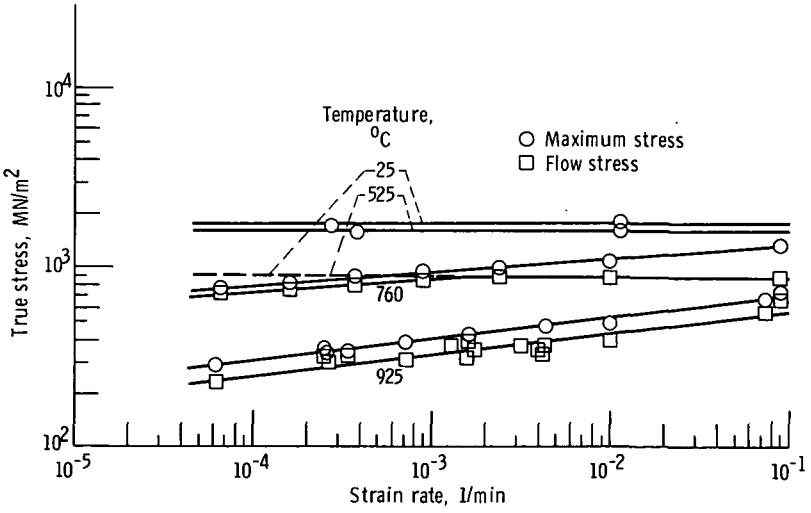

Figure 18. - Constant-strain-rate tensile strength data for Udimet 700.

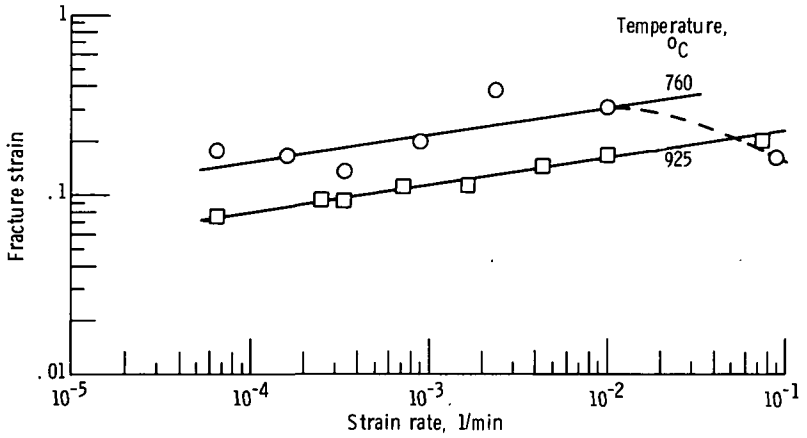

Figure 19. - Fracture strain of Udimet 700 at constant strain rate.

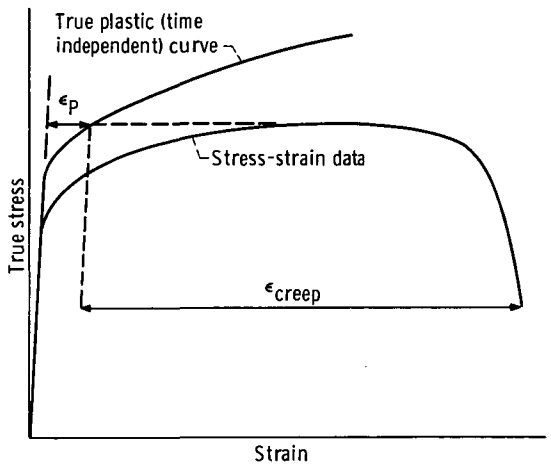

Figure 20. - Ductility-partitioning concept.

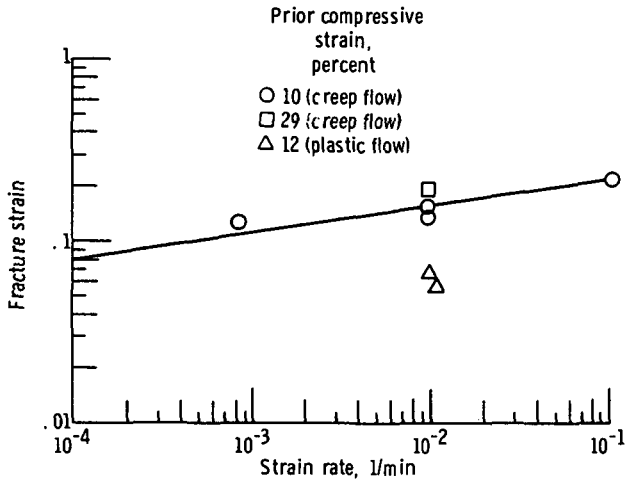

Figure 21. - Fracture strain of Udimet 700 at 925° C after prior compressive strain.

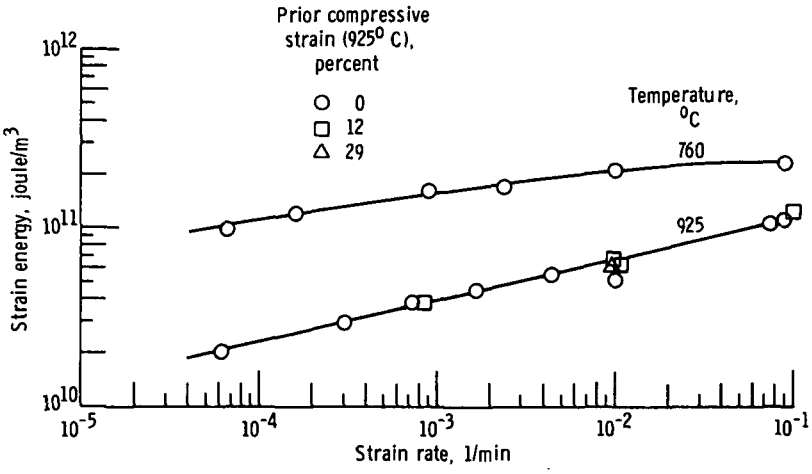

Figure 22. - Strain energy of Udimet 700 during constant-strain-rate tensile tests.

"The aeronautical and space activities of the United States shall be conducted so as to contribute . . . to the expansion of human knowledge of phenomena in the atmosphere and space. The Administration shall provide for the widest practicable and appropriate dissemination of information concerning its activities and the results thereof."

— NATIONAL AERONAUTICS AND SPACE ACT OF 1958

NASA SCIENTIFIC AND TECHNICAL PUBLICATIONS

TECHNICAL REPORTS: Scientific and technical information considered important, complete, and a lasting contribution to existing knowledge.

TECHNICAL NOTES: Information less broad in scope but nevertheless of importance as a contribution to existing knowledge.

TECHNICAL MEMORANDUMS: Information receiving limited distribution because of preliminary data, security classification, or other reasons.

CONTRACTOR REPORTS: Scientific and technical information generated under a NASA contract or grant and considered an important contribution to existing knowledge.

TECHNICAL TRANSLATIONS: Information published in a foreign language considered to merit NASA distribution in English.

SPECIAL PUBLICATIONS: Information derived from or of value to NASA activities. Publications include conference proceedings, monographs, data compilations, handbooks, sourcebooks, and special bibliographies.

TECHNOLOGY UTILIZATION PUBLICATIONS: Information on technology used by NASA that may be of particular interest in commercial and other non-aerospace applications. Publications include Tech Briefs, Technology Utilization Reports and Technology Surveys.

Details on the availability of these publications may be obtained from:

SCIENTIFIC AND TECHNICAL INFORMATION OFFICE

NATIONAL AERONAUTICS AND SPACE ADMINISTRATION

Washington, D.C. 20546